doi:10.1016/j.jmb.2006.05.014 J. Mol. Biol. (2006) 360, 421–434

JMB

Available online at www.sciencedirect.com

SCIENCE DIRECT®

ELSEVIER

Thermodynamics Reveal that Helix Four in the NLS of NF-κB p65 Anchors IκBα, Forming a Very Stable Complex

Simon Bergqvist[1], Carrie H. Croy[2], Magnus Kjaergaard[1], Tom Huxford[3] Gourisankar Ghosh[1] and Elizabeth A. Komives[1]*

[1]*Department of Chemistry and Biochemistry, University of California, San Diego 9500 Gilman Dr. La Jolla, CA 92093-0378, USA*

[2]*Department of Chemistry, University of Colorado, Boulder Boulder, CO 80309-0215, USA*

[3]*Department of Chemistry San Diego State University San Diego, CA 92182, USA*

**Corresponding author*

IκBα is an ankyrin repeat protein that inhibits NF-κB transcriptional activity by sequestering NF-κB outside of the nucleus in resting cells. We have characterized the binding thermodynamics and kinetics of the IκBα ankyrin repeat domain to NF-κB(p50/p65) using surface plasmon resonance (SPR) and isothermal titration calorimetry (ITC). SPR data showed that the IκBα and NF-κB associate rapidly but dissociate very slowly, leading to an extremely stable complex with a $K_{D,obs}$ of approximately 40 pM at 37 °C. As reported previously, the amino-terminal DNA-binding domain of p65 contributes little to the overall binding affinity. Conversely, helix four of p65, which forms part of the nuclear localization sequence, was essential for high-affinity binding. This was surprising, given the small size of the binding interface formed by this part of p65. The NF-κB(p50/p65) heterodimer and p65 homodimer bound IκBα with almost indistinguishable thermodynamics, except that the NF-κB p65 homodimer was characterized by a more favorable ΔH_{obs} relative to the NF-κB(p50/p65) heterodimer. Both interactions were characterized by a large negative heat capacity change ($\Delta C_{P,obs}$), approximately half of which was contributed by the p65 helix four that was necessary for tight binding. This could not be accounted for readily by the small loss of buried non-polar surface area and we hypothesize that the observed effect is due to additional folding of some regions of the complex.

Keywords: ankyrin repeat; isothermal titration colorimetry; rel family; IκBα; surface plasmon resonance

Introduction

In resting cells, NF-κB dimers with transcription activation potential are sequestered in the cytoplasm, interacting with a family of inhibitors of kappa B (IκBs) proteins.[1] The nuclear factor kappa B (NF-κB) is a family of transcription factors that control cellular signaling, cellular stress responses, cell growth, survival, and apoptosis.[2–5] It is known that at least 58 viral or bacterial products, some 46 stress conditions and chemicals, and at least 32 cytokines and receptor ligands, as well as apoptotic mediators and mitogens, activate the NF-κB signaling system and subsequently the expression of more than 150 target genes.[6] IκBα is capable of inhibiting many of the NF-κB family members, including the most abundant p50/p65, and other p65 and cRel-containing homo- and heterodimers.[3] Following the action of a large number of different stimuli, IκBα is phosphorylated, ubiquinylated, and degraded, freeing the NF-κB nuclear localization signal (NLS) which targets the NF-κB to the nucleus. In resting cells, the NF-κB/IκBα complex appears to be stable.[7] A hallmark of the NF-κB/IκBα complex is its high level of stability in resting cells, with a recent estimate of the IκBα half-life at longer than 48 h (A. Hoffmann *et al.*, unpublished results). This tight regulation is critical, as only a

Abbreviations used: NLS, nuclear localization signal; AR, ankyrin repeat; EMSA, electrophoretic mobility-shift assay; SPR, surface plasmon resonance; ITC, isothermal titration calorimetry.

E-mail address of the corresponding author: ekomives@ucsd.edu

small amount of NF-κB, due to leaky inhibition, is sufficient to give gene expression. This is confirmed by a recent study that showed that upon stimulation, only a small fraction of cytoplasmic NF-κB enters the nucleus and this results in transcriptional activation.[8]

The crystal structure of NF-κB(p50/p65) bound to IκBα was determined by two laboratories simultaneously (Figure 1(a)).[9,10] The structures reveal an extended protein–protein interface formed between IκBα and NF-κB, and provide a structural basis for the studies presented here. IκBα contains an ankyrin repeat domain, comprising six ankyrin repeat units, and a C-terminal PEST region. Each ankyrin repeat consists of about 33 residues and adopts a fold containing a β-hairpin, followed by two anti-parallel α- helices, followed by a short loop. The ankyrin repeat domain of IκBα forms an extensive interface with the NF-κB heterodimer, forming contacts in multiple regions (Figure 1(b)), and burying more than 4000 Å^2 of surface area in the interface. The two proteins run antiparallel with ankyrin repeat 1 (AR1) of IκBα, being capped by helix four of NF-κB p65 (residues 305–321). AR1–AR3 contact helix three (residues 289–300) of p65, and AR3–AR6 and the first part of the IκBα PEST sequence contact the NF-κB p50 and p65 dimerization domains. The PEST sequence also contacts the NF-κB p65 amino-terminal domain. Despite the structural and biochemical information locating the contacting surfaces, identification of the critical determinants of binding affinity has eluded us.[11] In this study, we address this important issue by taking apart the NF-κB/IκBα complex and carrying out a detailed study of the binding thermodynamics. We have previously investigated the interactions of the NF-κB dimers with IκBα by a fluorescence polarization competition assay,[12] and an electrophoretic mobility-shift assay (EMSA).[13] However, both techniques have potential limitations and so we have undertaken a more detailed study by direct binding assays using surface plasmon resonance (SPR) and isothermal titration calorimetry (ITC).

The binding thermodynamics and kinetics were measured for the interaction between IκBα and full-length NF-κB(p50/p65) heterodimer as well as with fragments of the NF-κB that were missing either the N-terminal domain or helix four from the NLS region. The interaction of IκBα with the p65 homodimer was also measured. These experiments helped to identify regions of NF-κB that are critical for tight binding affinity and they revealed the thermodynamics that drive the interaction.

We demonstrated previously that the free IκBα is highly dynamic in parts and only marginally stable in solution.[14] In the work presented here, we also measured the temperature-dependence of the binding interaction to investigate the possibility of a folding-upon-binding mechanism.

This study provides three important characteristics of the NF-κB/IκBα complex. First, the interaction has an extremely low dissociation rate, which results in very high affinity and explains the long half-life observed *in vivo*. Second, the affinity of the

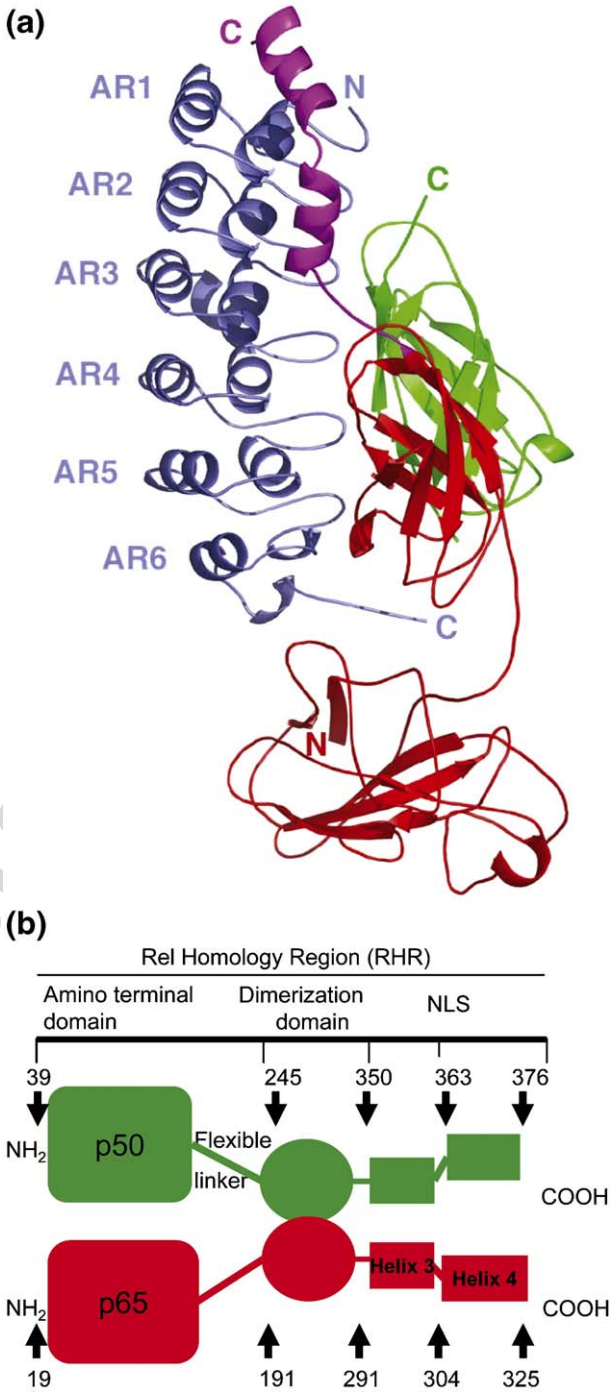

Figure 1. (a) Ribbon diagram showing the x-ray crystal structure of the NF-κB/IκBα complex. IκBα is colored blue. The NF-κB is colored to show the p50 subunit in green, the p65 RHR and dimerization domain in red and the p65 NLS and NLS extension in violet. This Figure was created using PyMOL v. 0.97 [http://pymol.sourceforge.net/] for the PDB coordinates (PDB accession code **1nfi**)[40]. (b) A schematic to show the domain structure of the NF-κB p50 (green) p65 (red) heterodimer.

interaction depends critically on the p65 NLS and this explains how the NLS is effectively sequestered by IκBα. Third, the thermodynamics help explain how IκBα can be very stable in complex with NF-κB and yet be degraded rapidly.

Results

IκBα forms a very stable complex with NF-κB

The binding kinetics and thermodynamics of the IκBα/NF-κB interaction were investigated by SPR. An N-terminal cysteine residue was introduced into NF-κB(p65) and the NF-κB($p50_{248-376}$/$p65_{19-325}$) heterodimer was biotinylated and immobilized on a streptavidin chip. Sensorgrams reveal that the IκBα/NF-κB interaction achieved high affinity by a combination of a fast association rate and a slow dissociation rate at 37 °C (Figure 2(a)) leading to a $K_{D,obs}$ of $3.9(\pm0.3)\times10^{-11}$ M (Table 1A). Experiments were carried out at 37 °C to speed the rate of dissociation of IκBα, which was very slow at 25 °C, relative to the baseline drift of the instrument. Even at 37 °C the dissociation rate was very low, which meant that we did not even begin to cover one half-life of the dissociation event within the 20 min dissociation period. Thus, the dissociation rate we report represents the upper limit of the true k_d and the true $K_{D,obs}$ for the complex may be even lower. Disruption of the NF-κB/IκBα complex required a 1 min pulse of 3 M urea at 37 °C and 6 M urea at 25 °C for regeneration. It is noteworthy that the NF-κB(p50/p65) heterodimer was tethered to the chip by only the p65 domain, and the non-covalent interactions between the p50 and p65 were not disrupted during regeneration, suggesting that they are very strong. SPR binding data showed that two different IκBα constructs comprising residues 67–287 or 67–317 bound to NF-κB with almost identical kinetics and affinity ($K_{D,obs}$ of $3.9(\pm0.3)\times10^{-11}$ M and $4.5(\pm1.0)\times10^{-11}$ M, respectively) (Table 1A) demonstrating that the C-terminal residues of IκBα, which extend the ''PEST'' sequence, do not have a significant effect on binding. Further experiments were performed using $IκBα_{67-287}$ because it was less prone to aggregation than the longer construct.

The NF-κB p65 amino-terminal DNA-binding domain contributes minimally to IκBα binding

The amino-terminal deletion construct, $p65_{190-321}$ (Figure 1(b)), was generated to investigate the effect of the p65 amino-terminal domain on IκBα binding. The heterodimer was formed using an excess (1000-fold) of un-tagged p50 and sensorgrams were obtained as for the NF-κB($p50_{248-376}$/$p65_{19-325}$), except that only a 1 min pulse of only 1.5 M urea was required for regeneration of the free NF-κB on the chip (Figure 2(b)). Comparison of the results from NF-κB($p50_{248-376}$/$p65_{19-325}$), which contained the amino-terminal domain of p65 (Table 1A) with results for NF-κB($p50_{248-350}$/$p65_{190-321}$), lacking the amino-terminal domain revealed an approximately twofold decrease in k_a and an approximate eightfold increase in k_d and a $K_{D,obs}$ of $3.2(\pm1.0)\times10^{-10}$ M (Table 1B). The faster dissociation rate permitted data to be recorded at 25 °C (Figure 2(c)) as well as 37 °C (Table 1B) for this complex. As expected, the dissociation rate was significantly slower at 25 °C resulting in a $K_{D,obs}$ of $0.91(\pm0.27)\times10^{-10}$ M.

Helix four of NF-κB p65 plays a major role in the slow dissociation rate of the complex

The C-terminal residues of NF-κB p65 contain the NLS consensus sequence KRKR at residues 301–304. This region is flanked by two α-helices, helix three (289–300) and helix four (305–321). Together, these motifs are known as the NLS domain (Figure 1(b)). We investigated the effect of helix four of the NLS on binding. Initial SPR experiments with NF-κB($p50_{248-350}$/$p65_{190-304}$) revealed that the IκBα dissociated orders of magnitude faster; too fast to be quantified at 37 °C. At 25 °C (Figure 3(a)) and at 15 °C (Figure 3(c)), the k_d of IκBα was $100(\pm20)\times10^{-3}$ s^{-1} and $24(\pm0.95)\times10^{-3}$ s^{-1}, respectively, compared to $0.12(\pm0.041)\times10^{-3}$ s^{-1} at 25 °C, for the longer construct (Table 1). Due to the weaker binding affinity, data were also analyzed by equilibrium analysis as shown in Figure 3(b) and (d), respectively. The results of the kinetic and equilibrium analyses were in good agreement, confirming the reliability of both modes of analysis. Thus, deletion of helix four of the p65 NLS resulted in an increase of more than 1000-fold in k_d. Including the decrease in k_a that was also observed, the affinity of IκBα for this complex was decreased by approximately 10,000-fold by the deletion of helix four of the NLS. Although the NF-κBs that contained helix four bound too tightly to measure the $K_{D,obs}$ accurately by ITC (Figure 2(d)), the NF-κBs that did not contain helix four bound weakly enough to allow direct comparison between the ITC and SPR data (Figure 4(a) and Table 2). The results showed good agreement between the two experiments, especially considering the complex nature of the two proteins involved. At 25 °C and 15 °C the $K_{D,obs}$ estimated by SPR was approximately four times and three times weaker, respectively, than that measured by ITC. The small discrepancy probably results from an effect of the surface change of the carboxymethyl dextran chip or of the linker used to immobilize the NF-κB. An electrostatic effect is more likely, since the IκBα contains an excess of acidic residues in its C-terminus. The ITC study confirmed the observation that the effect of the N-terminal domain on IκBα binding affinity is small (Table 2 and Figure 4(b)).

Since the NF-κB NLS appeared to be so important for binding, we generated synthetic peptides spanning the regions of the p65 NLS. Three peptides comprising residues 289–307, 289–314 and 289–320 were synthesized. Only the longest

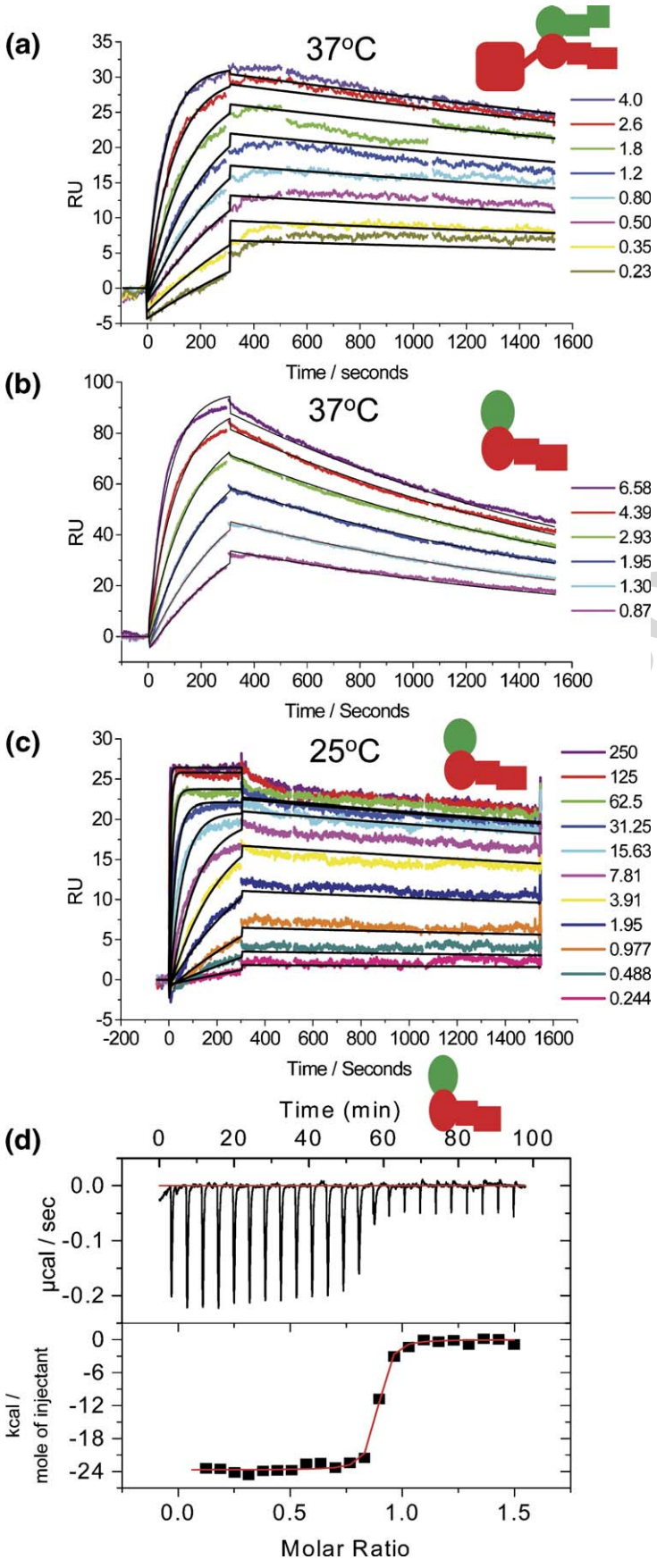

Figure 2. Summary of SPR data collected for the NF-κB/IκBα interaction. In all experiments, the NF-κB was immobilized to a streptavidin chip by a biotin tag on the p65 N terminus and IκBα was flowed over at a flow-rate of 50 µl/min. (a) Sensorgrams of 0.23–4.0 nM IκBα flowed over NF-κB($p50_{248-376}$/$p65_{19-325}$) at 37 °C. (b) Sensorgrams of 0.87–6.6 nM of IκBα flowed over NF-κB ($p50_{248-350}$/$p65_{190-321}$) at 37 °C. (c) Sensorgrams of 0.244–250 nM of IκBα flowed over NF-κB($p50_{248-350}$/$p65_{190-321}$) at 25 °C. (d) Binding isotherm of 50 µM NF-κB($p50_{248-376}$/$p65_{190-321}$) titrated in 5 µl injections into 3 µM IκBα. The buffer was 10 mM Mops (pH 7.5), 150 mM NaCl, 0.5 mM EDTA, 0.5 mM sodium azide and the temperature was 31 °C. Data were analyzed using a model for a single set of identical binding sites after the heat of dilution of NF-κB into buffer was subtracted. $K_{D,obs}$ was 2.2(±0.6) nM, and the stoichiometry was 0.9. The large error in K_D was due to the high c value for the interaction, where c is defined by Wiseman *et al.* and it is likely that affinity is significantly underestimated.[38]

Table 1. SPR kinetic and thermodynamic values for interactions between NF-κB and IκB constructs

A. *Interaction of NF-κB($p50_{248-376}$/$p65_{19-325}$) with IκBα(67-287) and IκBα(67-317)*

Interaction	k_a ($\times10^6$ $M^{-1}s^{-1}$)	k_d ($\times10^{-4}$ s^{-1})[a]	$K_{A,obs}$ ($\times10^{10}$ M^{-1})	$K_{D,obs}$ ($\times10^{-11}$ M)	X^2
67-287	3.7±0.16	1.5±0.16	2.5±0.36	3.9±0.30	1.0
67-317	3.3±0.60	1.4±0.55	2.2±0.10	4.5±1.0	0.7

B. *Interaction of NF-κB($p50_{248-350}$/$p65_{190-321}$) with IκBα(67-287) as a function of temperature*

Temp. (°C)	k_a ($\times10^6$ M^{-1} s^{-1})	k_d ($\times10^{-3}$ s^{-1})	$K_{A,obs}$ ($\times10^9$ M^{-1})	$K_{D,obs}$ ($\times10^{-9}$ M)	X^2
37	1.7±0.32	0.54±0.099	3.3±0.93	0.32±0.10	5.5
25	1.3±0.18	0.12±0.041	0.12±0.034	0.091±0.027	1.4

C. *Interaction of NF-κB($p50_{248-350}$/$p65_{190-304}$) with IκBα(67-287)*

25	0.24±0.08	100±20	0.0023±0.00056	460±120	0.43
15	0.15±0.01	24±0.95	0.0064±0.0005	158±12	0.28

D. *Interaction of NF-κB(p50/p65) heterodimer and NF-κB(p65/p65) homodimer binding to IκBα*

Interaction	k_a ($\times10^6$ M^{-1} s^{-1})	k_d ($\times10^{-3}$ s^{-1})	$K_{A,obs}$ ($\times10^9$ M^{-1})	$K_{D,obs}$ ($\times10^{-9}$ M)	X^2
p50p65[b]	1.7±0.32	0.54±0.10	3.3±0.93	0.32±0.10	5.5
p65p65[c]	2.9±0.30	1.6±0.14	1.9±0.25	0.54±0.08	0.45

Data were fit using the Biaevaluation 4.1 software to a simple Langmuir binding model. Experiments were carried out in triplicate for estimations of errors. In each experiment the amount of immobilized NF-κB was varied in the range of 50 to 400 RU.

[a] Since the dissociation rate was very low, we did not cover even a single half-life during the 20 min dissociation period. This means that the dissociation rate we determine represents the upper limit of the true k_d and the $K_{D,obs}$ for the complex may be even lower than we are able to determine.

[b] The construct used was NF-κB($p50_{248-350}$/$p65_{190-321}$) and $p65_{190-321}$/$p65_{190-321}$.

[c] The construct used was NF-κB($p65_{190-321}$/$p65_{190-321}$).

peptide, comprising residues 289–321, showed any detectable binding. An expressed version of this peptide that could be purified more readily bound with a $K_{D,obs}$ of 1.3(±0.09) × 10^{-6} M at 30 °C (Figure 5). The relatively tight binding affinity for such a short segment of NF-κB underscores the importance of the NLS for binding to IκBα. The observation that only peptides containing all of helix four bound IκBα again highlights the importance of this region of the NLS.

Helix four of p65 contributes half of the observed large negative $\Delta C_{P,obs}$ for IκBα/NF-κB (p50/p65) binding

Binding of NF-κB to IκBα was investigated over a range of temperatures using ITC. This technique provides a direct measure of the observed enthalpy change of binding (ΔH_{obs}) as well as the binding affinity. When carried out over a range of temperatures (at constant pressure), the observed heat capacity change ($\Delta C_{P,obs}$) and the full thermodynamic profile can be obtained. This was possible for the weaker binding IκBα/NF-κB($p50_{248-350}$/$p65_{190-304}$) complex, for which $K_{D,obs}$ and hence ΔG_{obs} and $T\Delta S_{obs}$ as well as the ΔH_{obs} could be determined accurately. The full thermodynamic profile for the interaction is shown in Figure 6(a). The compensation of ΔH_{obs} and $T\Delta S_{obs}$ leading to the relatively small change in ΔG_{obs} over the physiological temperature range is apparent from this plot.

For the IκBα/NF-κB($p50_{248-350}$/$p65_{190-321}$) complex containing the full NLS region, binding was too tight to permit determination of $K_{D,obs}$ directly. We were unable to employ a competition binding assay, due to the lack of a suitable competing ligand as used by Freire and co-workers,[15,16] and so only the ΔH_{obs} was determined for this interaction (Figure 6(b)). ΔH_{obs} was linear as a function of temperature up to approximately 33 °C, which is close to the temperature (45 °C) at which IκBα unfolds to a soluble aggregate.[14] Above 33 °C the slope curved as also reported by Ladbury and co-workers, for another interacting system.[17] As discussed later on, only the linear region of the plot was analyzed yielding a $\Delta C_{P,obs}$ = –1.30(±0.03) kcal mol^{-1} K^{-1}. This is a very large negative $\Delta C_{P,obs}$ even for such a large interaction interface suggesting additional contributions to the $\Delta C_{P,obs}$ that were not anticipated from the structure alone.

Comparison of the temperature-dependence of the formation of the two IκBα/NF-κB complexes, one with and one without helix four in the NLS, revealed that deletion of helix four resulted in a $\Delta C_{P,obs}$ of only –0.60(±0.03) kcal mol^{-1} K^{-1} compared to –1.30(±0.03) kcal mol^{-1} K^{-1} when helix four was present. This was a surprisingly large difference in $\Delta C_{P,obs}$ for such a small deletion from the C-terminus of NF-κB. Confirming these results, the $\Delta C_{P,obs}$ for the NLS peptide (residues 289–321) was measured to be –0.4(±0.04) kcal mol^{-1} K^{-1} (data not shown).

NF-κB(p50/p65) heterodimer and NF-κB(p65/p65) homodimer have an almost indistinguishable $K_{D,obs}$ and $\Delta C_{P,obs}$ for IκBα binding

Binding of the NF-κB(p65/p65) homodimer was measured by SPR to permit comparison with the heterodimer binding experiments. The NF-κB(p65/

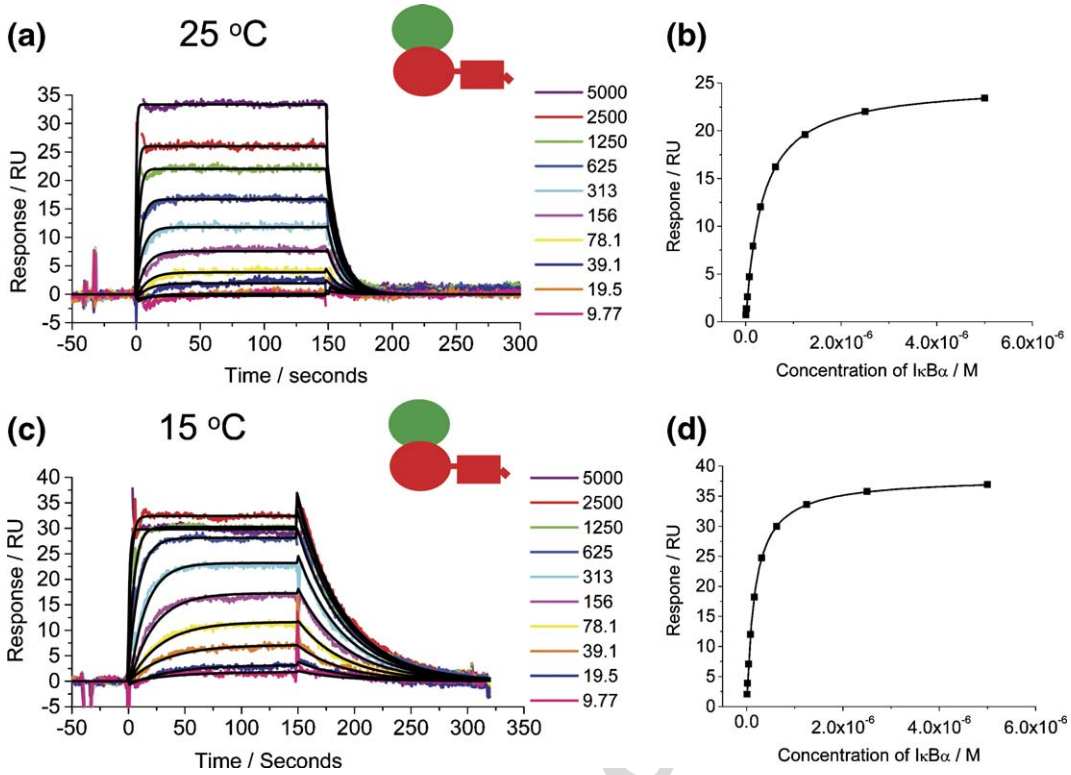

Figure 3. Summary of SPR data for the NF-κB($p50_{248-350}$/$p65_{190-304}$) from which the p65 helix four (305-321) was deleted. (a) Sensorgrams of 9.8–5000 nM concentrations of IκBα flowed over NF-κB at 25 °C kinetic analysis using a simple 1:1 model yielded $K_{D,obs}$ = 460(±120) nM. (b) Sensorgrams of 9.8–5000 nM concentrations of IκBα flowed over NF-κB at 15 °C. Kinetic analysis yielded $K_{D,obs}$ = 158(±12) nM. (c) Equilibrium analysis yielded $K_{D,obs}$ = 410(±100) nM. (d) Equilibrium analysis yielded $K_{D,obs}$ = 210(±93) nM. The equilibrium response was plotted against the concentration of IκBα and a line was fit to $I = K_A \times [I\kappa B\alpha]\ R_{max}/(K_A\ [I\kappa B\alpha]+1)$, where R is the equilibrium response at a specific concentration of IκBα, R_{max} is the response at saturation of the ligand on the chip, and $K_A = 1/K_D$.

p65) homodimer was immobilized on the chip by a single biotin linker on one of the p65 subunits. Analysis of the sensorgrams revealed binding characteristics almost indistinguishable from those for the NF-κB(p50/p65) heterodimer (Table 1D). The association rates were similar ($2.9(\pm0.3)\times10^6$ M^{-1} s^{-1} compared to $1.7(\pm0.32)\times10^6$ M^{-1} s^{-1}) as were the dissociation rates ($1.6(\pm0.14)\times10^{-3}$ s^{-1}compared to $0.54(\pm0.10)\times10^{-3}$ s^{-1}), leading to a less than twofold decrease in binding affinity for the p65 homodimer ($K_{D,obs} = 0.54(\pm0.08)\times10^{-9}$ M) relative to the heterodimer ($0.32(\pm0.10)\times10^{-9}$ M). This was also confirmed by the ITC data from the weaker binding complexes (Table 3). For example, $K_{D,obs}$ for the analogous heterodimer ($p50_{39-363}$/$p65_{1-304}$) and homodimer ($p65_{1-304}$/$p65_{1-304}$)/IκBα complexes were $42(\pm6.0)\times10^{-9}$ M and $51(\pm16)\times10^{-9}$ M, respectively. The ITC data showed also that IκBα binding to the NF-κB (p65/p65) homodimer is characterized by a large negative $\Delta C_{P,obs}$ ($\Delta C_{P,obs} = -1.43(\pm0.05)$ kcal mol^{-1} K^{-1}) similar to that observed for the NF-κB(p50/p65) heterodimer complex (Figure 7). Overall, the binding of IκBα to the homodimer is characterized by a more favorable (negative) ΔH_{obs} over the entire range of temperatures investigated, suggesting some compensation by a more unfavorable ΔS for the IκBα/homodimer complex.

Discussion

The IκBα/NF-κB complex is extremely high in affinity

The NF-κB signaling pathway is a complicated system involving a large number of protein/protein and protein/DNA interactions.[18] In order to have a complete understanding of the mechanism of regulation in this system, to understand the subtle effects mutations play, and to perhaps build models that predict the system-wide behavior,[19] it is essential that the thermodynamics and kinetics of each of the interactions be accurately determined. We have used two direct binding experiments to measure the contributions of the individual domains of p65 to the IκBα/NF-κB interaction. When the entire RHR of p65 was present, the binding affinity was approximately 40 pM, some 25-fold tighter than reported previously.[13] Previous measurements of the IκBα/NF-κB binding affinity using a fluorescence polarization competition assay and an electrophoretic mobility-shift assay, reported values of approximately 1 nM.[9,13] Both the ITC and the SPR data show that the affinity of NF-κB heterodimers and homodimers containing full-length p65 is much

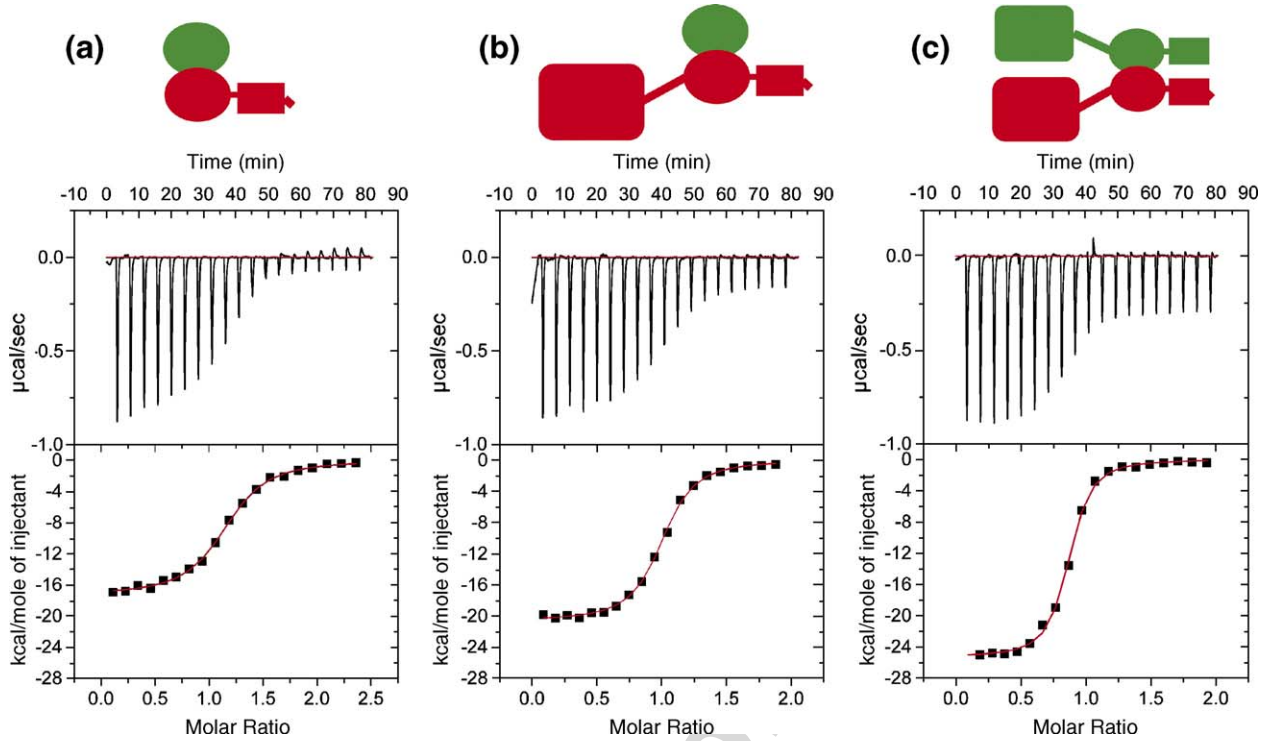

Figure 4. ITC binding isotherms for NF-κB binding to IκBα in 10 mM Mops (pH 7.5), 150 mM NaCl, 0.5 mM EDTA, 0.5 mM sodium azide at 30 °C. Experiments were carried out in triplicate and data were analyzed using a model for a single set of identical binding sites after the heat of dilution of NF-κB into buffer was subtracted. (a) NF-κB($p50_{248\text{-}350}$/$p65_{190\text{-}304}$), $K_{D,obs} = 333(\pm 21) \times 10^{-9}$ M, $n = 1.1 \pm 0.01$. (b) NF-κB($p50_{248\text{-}350}$/$p65_{1\text{-}304}$) $K_{D,obs} = 125(\pm 8) \times 10^{-9}$ M, $n = 0.99 \pm 0.02$. (c) NF-κB($p50_{39\text{-}363}$/$p65_{1\text{-}304}$) $K_{D,obs} = 42(\pm 6) \times 10^{-9}$ M, $n = 0.84 \pm 0.01$.

tighter than previously reported. The agreement between the present data and previously reported data is much better for the weaker binding complexes, suggesting that the EMSA and fluorescence polarization assays were simply underestimating the high affinity of the complexes containing the entire RHR of p65. In resting cells, the IκBα/NF-κB complex is in the cytoplasm awaiting stimulation of the IκB kinase that phosphorylates IκBα targeting it for ubiquitinylation and proteasome degradation.[3] Attempts to measure the intracellular half-life of the IκBα/NF-κB complex in resting cells report that the complex is exceedingly stable.[7] In IκB kinase knock-out cells, a half-life of at least 48 h and perhaps longer has been estimated (A. Hoffmann, unpublished results). Our observations that the affinity of the IκBα/NF-κB complex is in the picomolar range, and that the dissociation rate constant is so slow as to be nearly irreversible, are consistent with the long half-life that has been observed *in vivo*. This is a very important finding, because it helps to explain recent results showing that even upon activation, only a small fraction of the NF-κB is actually released from its inhibited state to translocate into the nucleus and turn on transcription.[8] The extremely high affinity of the inhibited complex ensures that there is no ''leakiness'' in this transcriptional inactivation system, and allows for rapid transcriptional activation upon release of inhibition.

Helix four within the NLS is predicted to contain important specific contact residues

We previously employed a structure-based mutagenesis approach to probe the interaction interface of the NF-κB/IκBα complex.[11] This investigation showed that when more than 20 residues of IκBα that form contacts with the NF-κB were mutated to alanine, only marginal effects on K_D were reported. This indicated a lack of a hot-spot in the NF-κB/IκBα interface. Mutations that made the most significant effects were that of Tyr181 to alanine, which makes contact to the p50 dimerization domain, and both Asp71 and Asp75 that make contact with Arg304 located between helix three and helix four in the NF-κB p65 NLS. When both residues are mutated to alanine, an approximate eightfold effect on binding of NF-κB was observed.[11] On the basis of the X-ray crystal structure, these residues seem to be important for anchoring the NLS. This agrees with our finding that truncation of the NLS by deletion of helix four has a large effect on the K_D of the complex, contributing one-third (4.5 kcal per mol) of the ΔG_{obs} at 25 °C (Table 4). The total surface area buried by this region is only one-sixth (818 Å compared to 4902 Å) of the total surface area buried by the whole RHR domain. The large contribution that this small region of p65 makes leads us to predict helix four within the p65 NLS (residues 305–320) will contain as yet unexplored

Table 2. Summary of SPR and ITC experiments probing C-terminal truncation of p65

Protein	Schematic	Temp . (° C)	$K_{D,obs\text{-}SPR}$ (x10^{-9} M)	$K_{D,obs\text{-}ITC}$ (x10^{-9} M)
$p50_{248\text{-}350}$/ $p65_{190\text{-}321}$		37	0.32±0.10	ND
$p50_{248\text{-}350}$/ $p65_{190\text{-}321}$		25	0.091±0.027	ND
$p50_{248\text{-}350}$/ $p65_{190\text{-}304}$		25	460±120	119±10
$p50_{248\text{-}350}$/ $p65_{190\text{-}304}$		30	ND	333±21
$p50_{248\text{-}350}$/ $p65_{1\text{-}304}$	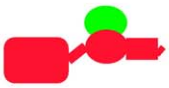	30	ND	125±8
$p50_{39\text{-}363}$/ $p65_{1\text{-}304}$		30	ND	42±6
$p50_{248\text{-}350}$/ $p65_{190\text{-}304}$		17	ND	57±6.1
$p50_{248\text{-}350}$/ $p65_{190\text{-}304}$		15	158±12	ND

SPR data were fit using the Biaevaluation 4.1 software to a simple Langmuir binding model. Experiments were carried out in triplicate for estimations of errors. In each experiment, the amount of immobilized NF-κB was varied in the range of 50–400 RU. The ITC data were fit to a model for a single set of identical binding sites after the heat of dilution of NF-κB into buffer was subtracted. The stoichiometry for the interaction was found to be consistent with a 1:1 binding model in all cases. For the SPR experiments, the experimental temperature depended on the dissociation rate for the interaction. For the very tight binding complexes at the top of the Table, the dissociation rate was too slow to be quantified at temperatures below 37 °C. For ITC experiments, the data could not be obtained easily at temperatures below 20 °C due to the small ΔH_{obs} and limitations of the instrument.

specific contact residues important for the tight binding affinity of the NF-κB/IκBα interaction. This finding is biologically significant, because tight binding of the NLS is expected to be important for sequestering the NLS from importin α. The KRKR sequence ending in Arg304 forms the essential recognition motif for the importin complex,[20–22] and a tightly bound helix four would most likely prevent specific interaction of the importin with the NLS.

The NF-κB p65 homodimer and NF-κB(p50/p65) heterodimer bind IκBα equally well, despite the difference in the dimerization domain interface

Consistent with previous results, our equilibrium and kinetic binding experiments have revealed that the ΔG_{obs} and $\Delta C_{P,obs}$ as well as the k_a and k_d for the NF-κB(p50p65) and the NF-κB(p65p65) binding to IκBα are almost identical.[13] Given that there are significant differences in the specific contacting residues between the p50p65 and the p65p65 with IκBα, there are two possible explanations for these results.[9] The residues that are not conserved in p50 relative to p65 might be isoenergetic or enthalpy/entropy-compensated in binding IκBα. This possibility is supported by the significantly more favorable ΔH_{obs} for the NF-κB(p65p65)/IκBα complex, which is compensated by a more unfavorable ΔS contribution relative to the NF-κB(p50p65)/IκBα complex. However, in the absence of a crystal structure of the p65p65/IκBα complex, it is difficult to rationalize this observation in detail. Another possible explanation is that the p65 subunit of the p50p65 contributes the major proportion of the ΔG_{obs} of binding and that the effect of subtle changes in contacting residues between the p50 subunit and the second p65 subunit in the homodimer/IκBα is not significant. This possibility is supported by our finding that the NLS of p65 contributes almost half of the overall affinity of the complex of NF-κB with IκBα.

These biophysical data are important, because they allow one to rationalize the biological effects of experiments, such as the p50 and p65 knock-out experiments in mice. Mice lacking the p50 subunit of NF-κB show no developmental abnormalities, apparently because the p65 homodimer can replace all of the important functions of the normally more abundant p50p65 heterodimer.[23] Conversely, the

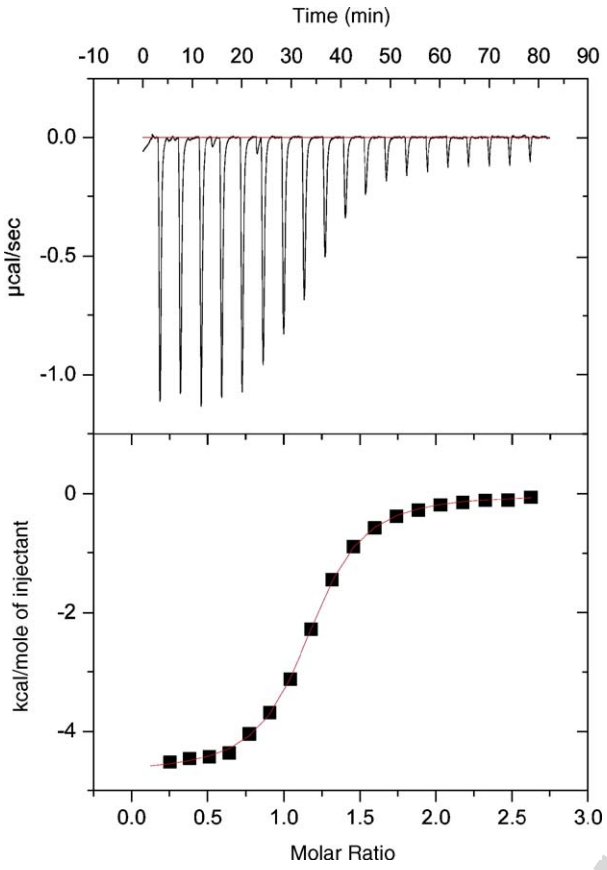

Figure 5. ITC binding isotherm for the peptide fragment of NF-κB p65(289-320) binding to IκBα in 10 mM Mops (pH 7.5), 150 mM NaCl, 0.5 mM EDTA, 0.5 mM sodium azide at 30 °C. Data were analyzed using a model for a single set of identical binding sites after the heat of dilution of NF-κB into buffer was subtracted a $K_{D,obs}$ of 1.3(±0.09)× 10^{-6} M and a stoichiometry of 1.1±0.05 at 30 °C was determined.

p65 knock-out is lethal in mice due to TNF-α induced apoptosis.[24] In normal cells, the NF-κB (p50p65) heterodimer is the most abundant form, but this is most likely due to increased expression levels of the p50 subunit or the increased affinity of the NF-κB (p50/p65) heterodimer compared to other dimers. Our results suggest that IκBα has evolved to recognize primarily p65 so that it can regulate gene expression by both p65p65 homodimers and by p50p65 heterodimers.

IκBα binding to the NF-κB dimer is characterized by a large negative $\Delta C_{P,obs}$

The variation of ΔH_{obs} for IκBα/NF-κB complex was linear over a temperature range of 17–33 °C (Figure 6(a)). At temperatures exceeding 33 °C, some negative curvature of the slope was observed (Supplementary Data Figure 1). A similar observation was reported recently by Ladbury and co-workers for the phosphate 5 tetratricopeptide repeat (TPR) domain with Hsp90.[17] These researchers were able to show that the non-linearity was due to an increased proportion of the unfolded form of the protein leading to an additional folding-coupled binding component of the ΔH_{obs}. It is also likely that the IκBα is unfolding in our experiments, since the unfolding transition for IκBα occurs around 45 °C.[14] Since the TPR domain reported by Ladbury and co-workers displayed reversible thermal unfolding behavior, the data were analyzed by simultaneously fitting unfolding data and the

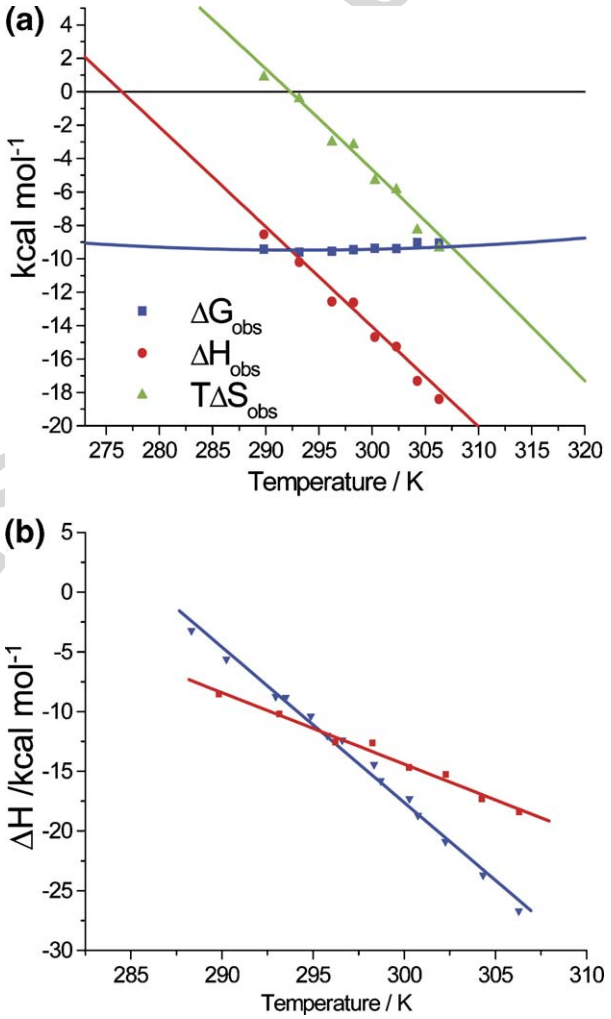

Figure 6. (a) Extrapolation of the thermodynamic characteristics of the NF-κB($p50_{248-350}/p65_{190-304}$)/IκBα interaction using the Gibbs-Helmholtz relation in the form: $\Delta G^{o}_{bind}(T_o) = \Delta H(T_o) - T_o[[\Delta H(T) - \Delta G^{o}(T)]/T + \Delta C_P \ln(T_o/T)]$, where ΔH is the enthalpy change, ΔG^{o}_{bind} is the free energy change upon binding, $T_o = 298$ K, and T is the absolute temperature. The ΔG_{obs} of the interaction is most favorable at approximately 20 °C when $T\Delta S_{obs} = 0$ (T_S). Since T_S occurs at the midpoint of the experimental range of temperatures investigated, the variation in $K_{D,obs}$ appears small compared to experimental error. (b) The temperature-dependence of ΔH_{obs} for the IκBα/NF-κB ($p50_{248-350}/p65_{190-321}$) (blue) and NF-κB-NLS truncation ($p50_{248-350}/p65_{190-304}$) (red) interaction. The slope of the line was used to determine $\Delta C_{P,obs} = -1.30 \pm 0.03$ for the full-length NLS and –0.60±0.03 for the NLS truncated NF-κB complex with IκBα.

Table 3. Comparison of NF-κB(p50/p65) heterodimer and NF-κB(p65/p65) homodimer binding data from SPR and ITC experiments

Protein	Schematic	Temp . (° C)	$K_{D\text{-}SPR}$ (x10^{-9} M)	$K_{D\text{-}ITC}$ (x10^{-9} M)
$p50_{248\text{-}350}$/ $p65_{190\text{-}321}$		37	0.32±0.10	ND
$p65_{190\text{-}321}$/$P65_{190\text{-}321}$		37	0.54±0.08	ND
$p50_{248\text{-}350}$/ $p65_{1\text{-}304}$		30	ND	125±8
$p65_{248\text{-}350}$/ $p65_{190\text{-}304}$		30	ND	320±28
$p50_{248\text{-}350}$/ $p65_{190\text{-}304}$		30	ND	330±23
$p50_{39\text{-}363}$/ $p65_{1\text{-}304}$	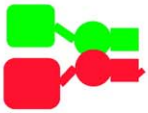	30	ND	42±6
$p65_{1\text{-}304}$/ $p65_{1\text{-}304}$		30	ND	51±16

SPR data were fit using the Biaevaluation 4.1 software to a simple Langmuir binding model. Experiments were carried out in triplicate for estimations of errors. In each experiment, the amount of immobilized NF-κB was varied in the range of 50–400 RU. ITC data were fit to a model for a single set of identical binding sites after the heat of dilution of NF-κB into buffer was subtracted. The stoichiometry for the interaction was found to be consistent with a 1:1 binding model in all cases. For the SPR experiments, the experimental temperature depended on the dissociation rate for the interaction. For the very tight binding complexes at the top of the Table, the dissociation rate was too low to be quantified at temperatures below 37 °C. For ITC experiments, the data could not be obtained easily at temperatures below 20 °C due to the small ΔH_{obs} and limitations of the instrument.

temperature-dependence of ΔH_{obs} as measured by ITC. Since IκBα displays irreversible thermal unfolding to an aggregate, we were able to fit only the linear part of the data. Determination of the $\Delta C_{P,obs}$ from the linear region of the curve has been shown to be a good approximation up to approximately 15 °C below the unfolding temperature of the protein, as was the case in our studies.[17] By this method, a relatively large $\Delta C_{P,obs}$ for IκBα binding (–1.30(±0.03) kcal mol^{-1} K^{-1}) was determined.

Many attempts have been made to relate $\Delta C_{P,obs}$ to burial of polar and non-polar surface area[25–28] and, more recently, including the burial of hydroxyl groups.[29] However, discrepancies commonly arise when folding or induced fit is coupled to binding, as in the case of many protein–DNA interactions,[28] or due to the presence of large numbers of buried water molecules,[30,31] or networks of water molecules near the surface of the interface.[32–34] While we cannot rule out any of these potential mechanisms leading to such a large $\Delta C_{P,obs}$, a model of folding-coupled binding of one or both binding partners could potentially account for the burial of non-polar surface area unanticipated from the structure of the complex. This is supported by our previous finding that parts of IκBα are highly dynamic in solution.[14]

A coupled folding and binding mechanism is consistent with the significant effect of removal of the fourth helix of p65 that caps ankyrin repeat 1 of IκBα. Indeed, removal of helix four in the NLS resulted in a halving of the $\Delta C_{P,obs}$. This was a surprisingly large difference in $\Delta C_{P,obs}$ for such a small deletion from the C-terminus of NF-κB. One likely explanation is that helix four ''caps'' ankyrin repeat 1 of IκBα effectively stabilizing the entire IκBα molecule. If this is the case, the effect of helix four binding may be propagated by strengthening contacts between neighboring repeats of the ankyrin repeat domain of IκBα resulting in a significant folding stabilization. This finding also has potential biological significance. With the tight association we observe for the IκBα/NF-κB complex, it then becomes difficult to imagine how the inhibition can be released rapidly upon IκB kinase activation

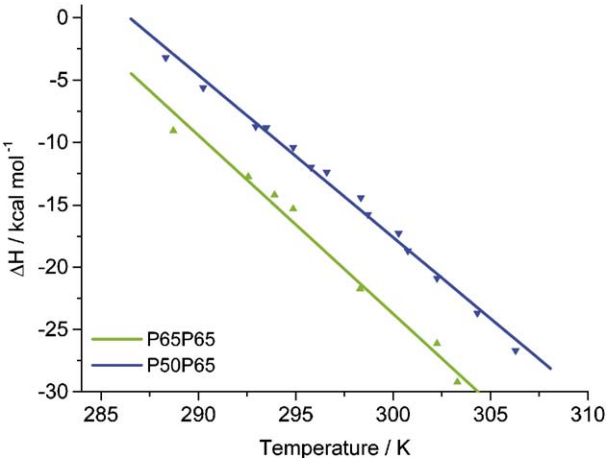

Figure 7. The temperature-dependence of ΔH_{obs} for the IκBα/NF-κB ($p50_{248-350}/p65_{190-321}$) (blue) and NF-κB p65 homodimer ($p65_{190-321}/p65_{190-321}$) (green) interaction. The trend shows that binding of the p65 homodimer to IκBα has a consistently more favorable ΔH_{obs} relative to the heterodimer over the experimental temperature range.

and proteasome targeting. Now one can imagine that the entire complex is brought to the proteasome, and that degradation occurs beginning with the unstructured N-terminal domain of IκBα. Subsequent degradation of the first ankyrin repeat will then result in the loss of the interaction between helix four of p65 and IκBα, followed by a 1000-fold increase in the k_d, resulting in rapid dissociation of the complex. The rest of IκBα could then be readily degraded and the NF-κB could then translocate to the nucleus. Thus, helix four may represent the key to unlock the tight complex between NF-κB and IκBα allowing for rapid transcriptional activation upon cellular stimulation.

Conclusion

Direct binding experiments have revealed, for the first time, the almost irreversible binding of IκBα to NF-κB. This helps explain the extremely long *in vivo* half-life of the complex and the leak-proof nature of the inhibition. The thermodynamics of the NF-κB/IκBα interaction, together with our previous studies of the dynamics of the free IκBα suggest that the IκBα/NF-κB interaction may involve coupled folding and binding. Deletion of helix four from the NLS of p65, which contacts the first ankyrin repeat of IκBα, increased the dissociation rate of the complex dramatically. This observation suggests a model whereby degradation of IκBα may only need to proceed through the first ankyrin repeat for complete and rapid NF-κB dissociation to occur.

Materials and Methods

Protein expression and purification

Human IκBα (67–287) was expressed in the Pet 11a vector and purified as described.[14] Two mutations were introduced into the p65 gene, N-terminal cysteine and a Cys38 to Ser to allow specific biotinylation only at the N terminus. This gene is referred to as p65. Murine NF-κB ($p50_{248-376}/p65_{19-325}$) was co expressed in a modified pET

Table 4. Summary of the free energy change (ΔG_{obs}) for different constructs of NF-κB p50p65 with IκBα

NF-κB	Schematic	Temp. (°C)	$\Delta SASA$ (Å)[a]	ΔG_{obs} (k cal mol^{-1})
$(p50_{248-376}/p65_{19-325})$	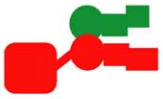	37	–4902	–14.7 (SPR)
$(p50_{248-350}/p65_{190-321})$		37	–4036	–13.5 (SPR)
$(p50_{248-350}/p65_{190-321})$		25	–4036	–13.9 (SPR)
$(p50_{248-350}/p65_{190-304})$		25	–3218	–9.4 (ITC)
$p65_{289-321}$		25	–1871	–7.5 (ITC)
$(p50_{248-350}/p65_{190-304})$		30	–3218	–9.9 (ITC)
$p65_{289-321}$		30	–1871	–8.2 (ITC)

[a] The ΔSASA (Å) was determined using the program GetArea 1.1 (http//www.scsb.utmb.edu/cgi-bin/get_a_form.tcl).[39]

29b vector and purified as described.[35] Cells were harvested and sonicated then centrifuged at 12,000 rpm (using an SS-34 rotor at 17,200***g***) for 45 min and the supernatant loaded onto a tandem fast flow Q and fast flow S column (GE Healthcare) equilibrated in 25 mM Tris (pH 7.5), 0.5 mM EDTA, 50 mM NaCl. After loading, the Q column was disconnected and protein fractions eluted from the S column with a gradient from 50 mM to 400 mM NaCl. Fractions were collected and analyzed by SDS PAGE. Bands were visualized by staining with silver and fractions of p50 and p65 with equal intensity were collected and pooled. The final step of the purification was size-exclusion chromatography on an S-200 Superdex column equilibrated in 10 mM Mops (pH 7.5), 0.5 mM EDTA, 150 mM NaCl, 0.5 mM sodium azide. The purified fractions were biotinylated by incubation with a 1:1 molar ratio of biotin PEO maleimide (Pierce Chemicals), at room temperature for 30 min and purified immediately by size-exclusion chromatography on an S200 Superdex 16/60 column. Fractions containing the biotinylated heterodimer were collected and stored at –80 °C in 50 μl portions.

All other NF-κB constructs were expressed using a Pet 11a single expression vector and purified using a similar tandem column technique. An N-terminal cysteine was introduced into the p65 as described above. For the NF-κB $p65_{190\text{-}321}$ and NF-κB $p50_{248\text{-}350}$ constructs, *Escherichia coli* BL21 DE3 cells were grown to an absorbance at 600 nm of 0.6 and induced at room temperature for 16 h with 0.1 mM IPTG. For the NF-κB $p65_{190\text{-}321}$ the column was equilibrated in 25 mM Mes (pH 7.0), 0.5 mM EDTA, 50 mM NaCl, 10 mM β-mercaptoethanol. For the NF-κB $p50_{248\text{-}350}$ the column was equilibrated in 25 mM Mes (pH 6.2), 0.5 mM EDTA, 50 mM NaCl, 10 mM β-mercaptoethanol, and a gradient of 50 mM–300 mM NaCl, was run.

For the NF-κB $p65_{1\text{-}325}$, NF-κB $p65_{1\text{-}304}$ and NF-κB $p50_{39\text{-}363}$ proteins, cells were induced with 0.5 mM IPTG. For NF-κB $p65_{1\text{-}325}$ the columns were equilibrated in 25 mM Mes (pH 6.5), 0.5 mM EDTA, 50 mM NaCl, 10 mM β-mercaptoethanol, a gradient was run from 50 mM–450 mM NaCl. For NF-κB $p65_{1\text{-}304}$ 25 mM Tris (pH 7.0), 0.5 mM EDTA 50 mM NaCl, 10 mM β-mercaptoethanol, and a 50 mM-300 mM NaCl gradient was used. For NF-κB $p50_{39\text{-}363}$ the columns were equilibrated in 25 mM Mes (pH 6.2), 0.5 mM EDTA, 50 mM NaCl, 10 mM β-mercaptoethanol and the gradient was run from 50 mM–700 mM NaCl.

Protein concentrations were determined spectrophotometrically from a scan of wavelengths 340-220 nm using the following ε_{280} values: 24,180 for NF-κB $p50_{248\text{-}350}$, 21,620 for NF-κB $p65_{190\text{-}321}$, 19,060 for NF-κB $p65_{190\text{-}304}$, 36,980 for the NF-κB $p65_{1\text{-}325}$, 34,420 for NF-κB $p65_{1\text{-}325}$, and 42,100 for NF-κB $p50_{39\text{-}363}$ homodimers and 30,580 for NF-κB($p50_{248\text{-}376}$/$p65_{19\text{-}325}$), 22,900 for NF-κB($p50_{248\text{-}350}$/$p65_{190\text{-}321}$), 21,620 for NF-κB($p50_{248\text{-}350}$/$p65_{190\text{-}304}$), 39540 for NF-κB($p50_{39\text{-}363}$/$p65_{1\text{-}325}$), 38,260 for NF-κB($p50_{39\text{-}363}$/$p65_{1\text{-}304}$) heterodimers. For $I\kappa B\alpha_{67\text{-}287}$ an ε_{280} of 12,090 was used. Dimers were formed *in vitro* by incubating an equimolar amount for 2 h at 25 °C and overnight at 4 °C before the ITC experiments. For SPR experiments, the p65 was biotinylated as already described. A 1000-fold excess of un-biotinylated p50 (for heterodimers) or p65 (for homodimers) was incubated with biotinylated p65 and the equilibrated mixture was immobilized immediately on a streptavidin (SA) SPR chip.

The C-terminal residues 289–321 of NF-κB were expressed in the trp leader vector, which contains a His_8 tag and thrombin cleavage sequence, and drives small peptides into inclusion bodies.[36] Inclusion bodies were solubilized with 6 M guanidine hydrochloride, 50 mM Tris (pH 7.4) and the solubilized peptide was captured by a Ni-NTA column equilibrated in the same buffer, and a gradient was run to a final concentration of 150 mM NaCl, 50 mM Tris (pH 7.4), 2 mM $CaCl_2$. The peptide was cleaved from the column with thrombin on the column for 4 h at 25 °C. The final purification step was reverse-phase HPLC on a C18 column with a 0–50% acetonitrile gradient, with 0.1% (v/v) TFA. The peptide was lyophilized and dissolved in 10 mM Mops (pH 7.5), 0.5 mM EDTA, 150 mM NaCl and the pH adjusted with 10 M NaOH.

SPR experiments

Sensorgrams were recorded on a Biacore 3000 instrument using streptavidin (SA) chips. Biotinylated NF-κB was immobilized on the chip in a high-salt buffer (500 mM NaCl, 10 mM Tris (pH 7.5), 0.5 mM EDTA, 0.5 mM sodium azide, 0.005% (v/v) P20). Sensorgrams were run in the automatic subtraction mode using flow-cell 1 (FC 1) as an unmodified reference. Data was collected for FC 2, FC3 and FC 4, which contained various amounts of NF-κB ligand with the lowest amount immobilized on FC 2 and the highest on FC 4. Injections were made using the kinject injection mode, alternating highest with lowest concentration samples, with a 5 min contact time and a 1200 s dissociation phase in all cases, except for the weaker interactions where a 3 min contact time and a 3 min dissociation phase were used. The running buffer used for the binding experiments was 10 mM Tris (pH 7.5), 0.2 mM EDTA, 150 mM NaCl, 10% (w/v) glycerol, 3 mM DTT, 0.5 mM sodium azide, 0.005% P20. The glycerol improved the stability of the NF-κB during regeneration. Regeneration was achieved using a 1 min pulse of a urea solution. The concentration of urea required depended on the NF-κB construct and the experimental temperature, and was prepared by diluting a 6 M stock into the running buffer. The minimum concentration of urea required for complete regeneration under each condition was determined by repeat injections. The data were analyzed using the Bia Evaluation 4.1 software using a simple 1:1 Langmuir binding model. Between three and 12 sensorgrams were obtained for each construct and condition tested using a range of concentrations of immobilized NF-κB.

For NF-κB($p50_{248\text{-}376}$/$p6519_{\text{-}325}$) at 37 °C, 200 RU, 300 RU and 400 RU of NF-κB were immobilized: 0.23–4.0 nM IκBα was injected. A 1 min pulse of 3 M urea was used for regeneration. Lower concentrations of ligand and analyte were not employed, to avoid the long-term noise of the instrument becoming significant relative to the slow dissociation of the IκBα.[37]

For NF-κB($p50_{248\text{-}350}$/$p65_{190\text{-}321}$), sensorgrams were obtained at 25 °C and 37 °C. NF-κB was immobilized at 50 RU, 75 RU, 100 RU, 150 RU, 200 RU, 250 RU and 350 RU. Sensorgrams were recorded using several ranges of IκBα. These were: 0.87– to 9.9 nM IκBα with 200 RU, 250 RU and 350 RU of NF-κB, 0.24 nM–20 nM IκBα for 50 RU, 75 RU and 100 RU of NF-κB and with 0.01–5 nM IκBα with 100 RU, 150 RU and 200 RU of NF-κB at 37 °C. For experiments at 25 °C, concentrations used were 0.87–9.9 nM IκBα with 100 RU, 200 RU and 300 RU of NF-κB, 0.24–20 nM and 0.022–10 nM IκBα with 50 RU, 75 RU and 100 RU of NF-κB. A 1 min pulse of 1.5 M urea was used for regeneration at 37 °C and 3 M urea at 25 °C.

For NF-κB($p50_{248\text{-}350}$/$p65_{19\text{-}304}$) at 25 °C, 16–1000 nM IκBα was used with 100 RU, 200 RU and 250 RU of NF-κB,

and 9.9–5000 nM IκBα was used with 50, 75 and 100 RU of NF-κB. At 15 °C, 9.9–5000 nM IκBα was used with 50 RU, 75 RU and 100 RU of NF-κB. No regeneration was required at either temperature with this NF-κB construct because it bound so weakly. Data were analyzed by equilibrium analysis in addition to the kinetic analysis. The equilibrium response was plotted against the concentration of IκBα and fit to:

$$R = K_A[I\kappa B\alpha]R_{max}/(K_A[I\kappa B\alpha] + 1)$$

where R is the equilibrium response at a specific concentration of IκBα, R_{max} is the response at saturation of the ligand on the chip, and $K_A = 1/K_D$.

For the NF-κB($p50_{248-350}$/$p65_{19-304}$), the effect of the 10% glycerol in the running buffer was assessed by experiments at 25 °C with 9.9–5000 nM IκBα and 50 RU, 75 RU and 100 RU of NF-κB immobilized using a running buffer that was the same as that used for the ITC experiments (10 mM MOPS (pH 7.5), 0.5 mM EDTA, 150 mM NaCl, 0.5 mM sodium azide, 0.005% p20). No significant difference in the binding data was observed using this buffer.

ITC experiments

ITC experiments were carried out on a Microcal MCS instrument. IκBα and NF-κB were purified by size-exclusion chromatography on an S-75 or S-200 column, respectively, immediately before use. In a typical ITC experiment, 20 injections of 15 μl of 50 μM NF-κB were made into a 5 μM IκBα solution in the cell. ITC experiments were carried out in a buffer of 10 mM MOPS (pH 7.5), 0.5 mM EDTA, 150 mM NaCl, 0.5 mM sodium azide. Isotherms were analyzed using the Origin software (Microcal) as described.[38] For the very tight complexes, the $K_{D,obs}$ could not be determined due to the high c value for the interaction, where c is defined by Wiseman *et al*.[38]

Surface area calculations

Surface area calculations were carried out using the Getarea 1.1 program†.[39]

Supplementary Data

Supplementary data associated with this article can be found, in the online version, at doi:10.1016/j.jmb.2006.05.014

References

1. Karin, M. & Ben-Neriah, Y. (2000). Phosphorylation meets ubiquitination: the control of NF-[kappa]B activity. *Annu. Rev. Immunol.* **18**, 621–663.
2. Baldwin, A. S. (1996). The NF-kappa-B and I-kappa-B proteins: new discoveries and insights. *Annu. Rev. Immunol.* **87**, 13–20.
3. Baltimore, D., Alcarno, E., Hoffmann, A. & Stankovski, I. (1999). NF-kB's many facets. *FASEB J.* **13**, A1429.
4. Gerondakis, S., Grossmann, M., Nakamura, Y., Pohl, T. & Grumont, R. (1999). Genetic approaches in mice to understand Rel/NF-kappaB and IkappaB function: transgenics and knockouts. *Oncogene*, **18**, 6888–6895.
5. Ghosh, S., May, M. J. & Kopp, E. B. (1998). NF-kappa B and Rel proteins: evolutionarily conserved mediators of immune responses. *Annu. Rev. Immunol.* **16**, 225–260.
6. Pahl, H. L. (1999). Activators and target genes of Rel/NF-kappaB transcription factors. *Oncogene*, **18**, 6853–6866.
7. Pando, M. P. & Verma, I. M. (2000). Signal-dependent and -independent degradation of free and NF-kappa B bound IkappaBalpha. *J. Biol. Chem.* **275**, 21278–21286.
8. Tergaonkar, V., Correa, R. G., Ikawa, M. & Verma, I. M. (2005). Distinct roles of IkappaB proteins in regulating constitutive NF-kappaB activity. *Nature Cell Biol.* **7**, 921–923.
9. Huxford, T., Huang, D. B., Malek, S. & Ghosh, G. (1998). The crystal structure of the I kappa B alpha/NF-kappa B complex reveals mechanisms of NF-kappa B inactivation. *Cell*, **95**, 759–770.
10. Jacobs, M. D. & Harrison, S. C. (1998). Structure of an I kappa B alpha/NF-kappa B complex. *Cell*, **95**, 749–758.
11. Huxford, T., Mishler, D., Phelps, C. B., Huang, D. B., Sengchanthalangsy, L. L. Reeves, R. *et al.* (2002). Solvent exposed non-contacting amino acids play a critical role in NF-kappa B/IkB alpha complex formation. *J. Mol. Biol.* **324**, 587–597.
12. Malek, S., Huxford, T. & Ghosh, G. (1998). IkBa functions through direct contacts with the nuclear localization signals and the DNA binding sequences of NF-kB. *J. Biol. Chem.* **273**, 25427–25435.
13. Phelps, C. B., Sengchanthalangsy, L. L., Huxford, T. & Ghosh, G. (2000). Mechanism of I kappa B alpha binding to NF-kappa B dimers. *J. Biol. Chem.* **275**, 29840–29846.
14. Croy, C. H., Bergqvist, S., Huxford, T., Ghosh, G. & Komives, E. A. (2004). Biophysical characterization of the free IkappaBalpha ankyrin repeat domain in solution. *Protein Sci.* **13**, 1767–1777.
15. Sigurskjold, B. W. (2000). Exact analysis of competition ligand binding by displacement isothermal titration calorimetry. *Anal. Biochem.* **277**, 260–266.
16. Velazquez-Campoy, A., Kiso, Y. & Freire, E. (2001). The binding energetics of first- and second-generation HIV-1 protease inhibitors: Implications for drug design. *Arch. Biochem. Biophys.* **390**, 169–175.
17. Cliff, M. J., Williams, M. A., Brooke-Smith, J., Barford, D. & Ladbury, J. E. (2005). Molecular recognition via coupled folding and binding in a TPR domain. *J. Mol. Biol.* **346**, 717–732.
18. Hoffmann, A., Leung, T. H. & Baltimore, D. (2003). Genetic analysis of NF-kB/Rel transcription factors defines functional specificities. *EMBO J.* **22**, 829–839.
19. Hoffmann, A., Levchenko, A., Scott, M. L. & Baltimore, D. (2002). The IkappaB-NF-kappaB signaling module: temporal control and selective gene activation. *Science*, **298**, 1241–1245.
20. Dang, C. V. & Lee, W. M. F. (1988). Identification of the human C-Myc protein Nuclear translocation signal. *Mol. Cell. Biol.* **8**, 4048–4054.
21. Dingwall, C. & Laskey, R. A. (1991). Nuclear targeting sequences - a consensus. *Trends Biochem. Sci.* **16**, 478–481.
22. Leung, S. W., Harreman, M. T., Hodel, M. R., Hodel, A. E. & Corbett, A. H. (2003). Dissection of the karyopherin alpha nuclear localization signal (NLS)-

† www.scsb.utmb.edu/cgi-bin/get_a_form.tcl

binding groove - functional requirements for NLS binding. *J. Biol. Chem.* **278**, 41947–41953.
23. Sha, W. C., Liou, H. C., Tuomanen, E. I. & Baltimore, D. (1995). Targeted disruption of the P50 subunit of Nf-Kappa-B leads to multifocal defects in immune-responses. *Cell*, **80**, 321–330.
24. Beg, A. A. & Baltimore, D. (1996). An essential role for NF-kappa B in preventing TNF-alpha-induced cell death. *Science*, **274**, 782–784.
25. Ha, J. H., Spolar, R. S. & Record, M. T. (1989). Role of the hydrophobic effect in stability of site-specific protein-DNA complexes. *J. Mol. Biol.* **209**, 801–816.
26. Livingstone, J. R., Spolar, R. S. & Record, M. T. (1991). Contribution to the thermodynamics of protein folding from the reduction in water-accessible non-polar surface-area. *Biochem.* **30**, 4237–4244.
27. Spolar, R. S., Livingstone, J. R. & Record, M. T. (1992). Use of liquid-hydrocarbon and amide transfer data to estimate contributions to thermodynamic functions of protein folding from the removal of nonpolar and polar surface from water. *Biochemistry*, **31**, 3947–3955.
28. Spolar, R. S. & Record, J. M. T. (1994). Coupling of local folding to site-specific binding of proteins to DNA. *Science*, **263**, 777–784.
29. Murphy, K. P. & Freire, E. (1992). Thermodynamics of structural stability and cooperative folding behavior in proteins. *Advan. Protein Chem.* **43**, 313–361.
30. Ladbury, J. E., Wright, J. G., Sturtevent, J. M. & Sigler, P. B. (1994). A thermodynamic study of the trp repressor-operator interaction. *J. Mol. Biol.* **238**, 669–681.
31. Morton, C. J. & Ladbury, J. E. (1996). Water-mediated protein-DNA interactions: the relationship of thermodynamics to structural detail. *Protein Sci.* **5**, 2115–2118.
32. Bergqvist, S., Williams, M. A., O'Brien, R. & Ladbury, J. E. (2004). Heat capacity effects of water molecules and ions at a protein–DNA interface. *J. Mol. Biol.* **336**, 829–842.
33. Baker, B. M. & Murphey, K. P. (1996). Evaluation of linked protonation effects in protein binding reactions using isothermal titration calorimetry. *Biophys. J.* **71**, 2049–2055.
34. Bradshaw, J. M. & Waksman, G. (1998). Calorimetric investigation of proton linkage by monitoring both the enthalpy and association constant of binding: application to the interactionof the Src SH2 domain with a high affinity tyrosyl phosphopeptide. *Biochemistry*, **37**, 15400–15407.
35. Chen, F. E., Kempiak, S., Huang, D. B., Phelps, C. & G., G. (1999). Construction, expression, purification and functional analysis of recombinant NFkappaB p50/p65 heterodimer. *Protein Eng.* **12**, 423–428.
36. North, C. L. & Blacklow, S. C. (2000). Evidence that familial hypercholesterolemia mutations of the LDL receptor cause limited local misfolding in an LDL-A module pair. *Biochemistry*, **39**, 13127–13135.
37. Rich, R. L. & Myszka, D. G. (2005). Survey of the year 2004 commercial optical biosensor literature. *J. Mol. Recogn.* **18**, 431–478.
38. Wiseman, T., Williston, S., Brandts, J. F. & Lin, L. N. (1989). Rapid measurement of binding constants and heats of binding using a new titration calorimeter. *Anal. Biochem.* **179**, 131–137.
39. Fraczkiewicz, R. & Braun, W. (1998). Exact and efficient analytical calculation of the accessible surface areas and their gradients for macromolecules. *J. Comput. Chem.* **19**, 319–333.

Edited by J. E. Ladbury

(Received 6 February 2006; received in revised form 5 April 2006; accepted 5 May 2006)
Available online 19 May 2006